World Academy of Science, Engineering and Technology
International Journal of Physical and Mathematical Sciences
Vol:19, No:2, 2025

Empirical Validation of Rotational Lorentz Transformations: Insights into Particle Spin, Field Energy, the Origins of Mass and Dark Matter

Rui Yin, Ming Yin, Yang Wang

***Abstract*—**This paper presents empirical evidence supporting the Lorentz transformation for rotational frames in both inside critical cylinder (ICC) and outside critical cylinder (OCC) configurations, alongside the corresponding transformations of related physical quantities. These transformations are applied to derive the electromagnetic field parameters of a spinning charged particle. Our analysis of the particle's field energy not only reveals the masses of the proton and electron but also uncovers the underlying mechanism that accounts for the significant mass disparity between them. Additionally, we explore the relationship between the energy interval and the angular velocity of the spinning particle. Our results provide a deeper understanding of the nature of particle mass and may offer important insights into the study of dark energy and dark mass.

***Keywords*—**Special Relativity, Lorentz Transformation. field energy, particle spin, dark mass, dark energy.

I. Introduction

FOR the fixed axis rotation, the relation between the tangential velocity v, angular velocity ω, and the radial distance r have $v = r\omega$. Therefore, any rotation has a corresponding radial distance r_c, where v reaches the speed of light c:

$$r_c\omega = c, i.e., r_c = c/\omega$$

We define r_c the critical radius. All points at a radial distance of r_c from the center form an infinitely long cylindrical surface, referred to as the critical cylinder. It has been previously assumed that v at the OCC is superluminal, which is considered impossible according to the principles of special relativity. However, our experiments demonstrate that there are distinct natural laws governing the OCC and the ICC. Contrary to previous assumptions, we show that the tangential velocity at the OCC is, in fact, subluminal.

II. Experimental Observation of Rotation Relativistic Effects

A. Experimental Scheme

When the spin magnetic moment (M) of a charged particle is not aligned with the external magnetic field (B), the field cause the magnetic moment to precess, aligning it parallel to the field. The relationship between the precession angular velocity ω_m and B is given by the equation: $\omega_m = 2\pi\gamma B$, where γ is the gyromagnetic ratio. For free electrons, γ_e is 2.6667×10^{-10} Hz/Tesla. For a magnetic field strength of B = 0.12 Tesla, the precession angular velocity ω_m is calculated to be 2.0106×10^{10} rad/s, and the corresponding critical radius r_c is approximately 1.5 cm, which facilitates the direct observation of the electric force exerted on the precessing electrons.

B. Experimental Setup, Methods, and Results

A helical electrode, 15 mm in length and 2 mm in diameter, is connected to the negative output terminal of a high DC voltage generator (HVG) with an 1,800 V_{DC} output. The electrode is fixed to the resin surface of a single-sided copper-clad laminate board, which is secured within a plastic dish. The two ends of two U-type ferrite cores (Mn-Zn 2000) clamp the electrode, the resin plate, and the plastic dish together, while the other two ends are inserted into the exciting coil consisting of 1600 turns (2×800 turns), as illustrated in Fig. 1: When the HVG is activated, a significant accumulation of free electrons forms on the surface of the electrode.

A square wave current generator (SWCG) with an adjustable output current range of 0.4 A to 0.6 and a period of 10 μS period (80% duty cycle) supplies current to the coil, generating a magnetic field that is transferred to the electrode through two ferrite cores. This magnetic field induces precession of the free electrons on the electrode surface. By varying the amplitude of the square wave current, the magnetic field strength (*B)* f passing through the electrons can be adjusted, thereby modifying the critical radius (r_c). Initially, B is set to 0.12 Tesla, which results in a precession critical radius (r_c) of 1.492 cm for the electrons. A 20% carbon ink, containing a high concentration of anionic surfactants (negatively charged ions), is employed as the test charge.

First, warm water is added to the plastic dish, and a small amount of ink is injected 1 cm to 1.3 cm to the right side of the electrode. The HVG is then activated, causing the generation of electrons on the electrode's surface. As a result, the ink is repelled to the right, as demonstrated in the four sequential screenshots from the video shown in Fig. 2 (b).

Rui Yin is with Beihang University, Beijing, China 100191 (phone: +86-13051343464; e-mail: yr195@ buaa.edu.cn).

Ming Yin is with Beihang University, Beijing, China 100191 (e-mail: 2320314608@qq.com).

Yang Wang was with Beihang University, Beijing, China 100191.He is now with RF Lab (Hongkong) Limited, Hong Kong, China (corresponding author, phone: +86-13003429159 e-mail: thomasyang.wang@gmail.com).

a) Electrode is connected with HVG

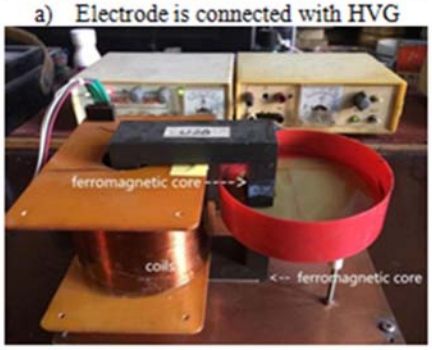

b) **Two ferromagnetic cores clamp electrode**

Fig. 1 The experimental setup

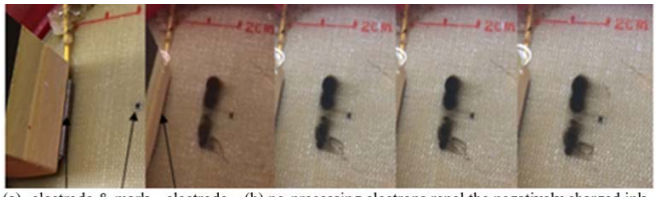

(a) electrode & mark electrode (b) no-precessing electrons repel the negatively charged ink

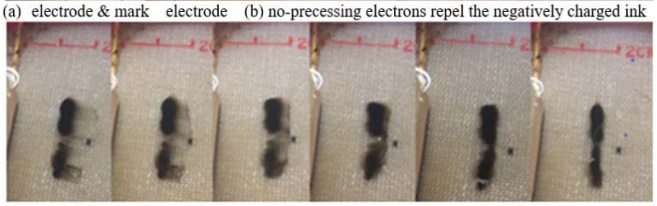

(c) precessing electrons exert repulsion on the ink of ICC but attraction on the ink of OCC

Fig. 2 Ten screenshots from the experimental video

Once the right edge of the ink is repelled to the black mark (the center of the resin board), the SWCG is activated to induce precession of the electrons. As a result, the left edge of the ink continues to be repelled to the right, while the right edge begins to be attracted to the left by the precessing electrons. Fig. 2 (c) presents six sequential screenshots from the video. The full video is available on YouTube [1].

The experimental results show that the electric force of precessing electrons exists in the OCC and is directed opposite to that in the ICC. This opposite electric force in the OCC represents a newly discovered natural law.

To observe the change in the electric force acting on the electrons on either side of the critical radius (r_c), a red line is drawn 1.5 cm away from the electrode. The experiment is then repeated, and the results are shown in Figs. 3 and 4, which display video screenshots from the repeated experiment. Figs. 3 (a) and 4 (a) show two sequential screenshots illustrating the repulsive force exerted on the ink by the electrons when no magnetic field (B) is applied, causing the ink to be repelled to the right. Figs. 3 (b) and 4 (b) present five sequential screenshots after the magnetic field is applied. In this case, the precessing electrons attract the ink on the right side of the red line, while the ink on the left side of the red line is gradually repelled to the right. These observations demonstrate that precessing electrons attract negative charges in the OCC and repel those in the ICC.

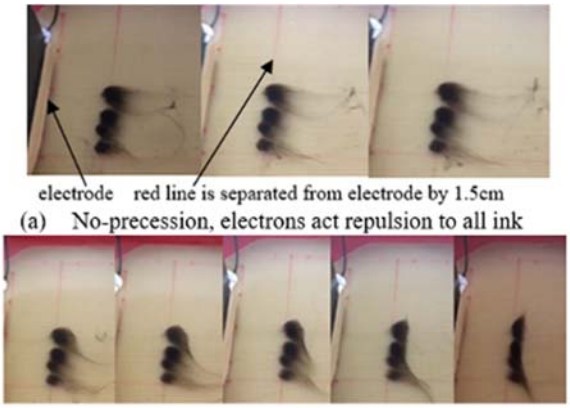

(a) No-precession, electrons act repulsion to all ink

(b)Precessing electrons act both repulsion and attraction to the ink separated by the critical radius of precession

Fig. 3 The screenshots of the experimental video as B is 0.12 T and r_c is 1.5 cm

(a) No-precessing electron act repulsion to all ink the vertical red line is separated from the electrode by 1.5cm

electrode

(b) The precessing electrons act both repulsion to the ink at ICC and attraction to the ink at OCC

Fig. 4 Screenshots of the experimental video as B is 0.12 T and r_c is 1.5 cm

Furthermore, increasing the magnetic field strength (B) to 0.13 Tesla results in a precession angular velocity (ω_m) of 2.1728×10^{10} rad/s and a critical radius (r_c) of 1.377 cm. Fig. 5 displays 12 sequential screenshots from the video. Fig. 5 (a) shows four screenshots of the ink moving to the right of the red line (1.5 cm from the electrode), due to the repulsive force exerted by non-precessing electrons. Fig. 5 (b) presents eight sequential screenshots illustrating that, with precessing electrons, the ink to the right of the red line is attracted leftward, eventually gathering at the right side of r_c (1.377 cm) from the electrode, while remaining to the left of the red line.

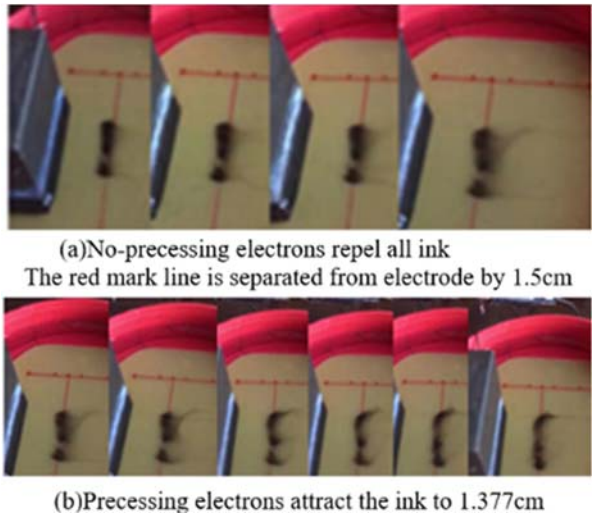

Fig. 5 Screenshots of the experimental video as B is 0.13 T and r_c is 1.377 cm

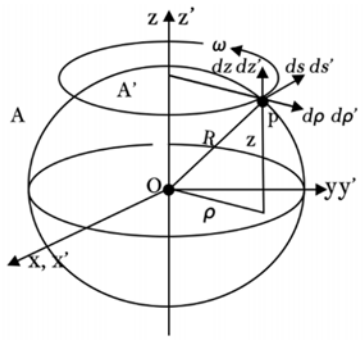

Fig. 6 Local reference frame of point P

C. Experimental Results Discussion

This experiment reveals a discovered natural law: the electric force of precessing electrons exists in the OCC, but its direction is opposite to that in the ICC. In fact, many physical quantities associated with rotation exhibit reversed mathematical signs in the OCC compared to the ICC. This reversal occurs when charges rotate, representing a relativistic rotational effect that we term the Critical Cylinder Effect (CCE). The CCE highlights the incompleteness of Coulomb's law, which was formulated prior to the discovery of electron spin.

Moreover, the observed critical radius suggests that electron precession is a rotation with a well-defined axis and constant tangential velocity. Since only a rotating object can exhibit precession when subjected to an external torque, electron spin therefore represents a rotation with a fixed axis and constant angular velocity. In addition, quantum mechanics postulates that the electric force is mediated by photons, meaning that electrons emit (virtual) photons that interact with negative ions, thereby causing a change in the momentum of these ions. The rate of momentum change corresponds to the force exerted on the negative ions [2]. However, this explanation fails to account for why photon exchanges would result in opposing forces on either side of the critical radius. The electric force must interact with a medium rotating in synchrony with the precession, rather than being mediated by (virtual) photons.

The existence of the electric field force in the OCC implies that the tangential velocity of the electric field of precessing electrons does not exceed the speed of light in the OCC. In fact, the relationship between the tangential velocity (v) and angular velocity (ω) for fixed-axis rotation in the OCC is no longer expressed as $v = r\omega$, but rather as $v = c^2/(r\omega)$. The theoretical proof of this relationship is presented in Section III.

III. Space-Time Exchange and Tangential Velocity of Rotation

We assume that the two reference frames A and A' rotate around the z(z') axis at an angular velocity ω relative to each other, as illustrated in Fig. 6. By substituting the differentials of arc length (ds), radial distance ($d\rho$), axial distance (dz), and time (dt) at the observed point P into the Cartesian coordinates and time (x,y,z,t), the Lorentz transformation and its inverse between the rotating frames are given by the following equations [3], [4]:

$$\begin{cases} ds' = \gamma(ds - \rho\omega dt) \\ d\rho' = d\rho \\ dz' = dz \\ dt' = \gamma\left(dt - \frac{\rho\omega}{c^2}ds\right) \end{cases} \tag{1}$$

$$\begin{cases} ds = \gamma(ds' + \rho\omega dt') \\ d\rho = d\rho' \\ dz = dz' \\ dt = \gamma\left(dt' + \frac{\rho\omega}{c^2}ds'\right) \end{cases} \tag{2}$$

where,

$$\gamma = \frac{1}{\sqrt{1-\frac{\rho^2\omega^2}{c^2}}} \tag{3}$$

However, they are only valid for ICC. For OCC, with the $d\rho' = d\rho$ and $dz' = dz$ are maintained, we only explore the first and last equations of (2). These equations are:

$$\begin{cases} ds = \gamma(ds' + \rho\omega dt') \\ dt = \gamma\left(dt' + \frac{\rho\omega}{c^2}ds'\right) \end{cases} \tag{4}$$

Note $\gamma = \frac{1}{\sqrt{1-\rho^2\omega^2/c^2}} \cdot \frac{c/(\rho\omega)}{c/(\rho\omega)} = \begin{cases} \frac{c}{\rho\omega} \cdot \frac{1}{\sqrt{\frac{c^2}{\rho^2\omega^2}-1}} \cdot \frac{i}{i} \\ \frac{c}{\rho\omega} \cdot \frac{1}{i\sqrt{1-\frac{c^2}{\rho^2\omega^2}}} \cdot \frac{i}{i} \end{cases} =$

$\begin{cases} \frac{ic}{\rho\omega} \cdot \frac{1}{\sqrt{1-c^2/(\rho^2\omega^2)}} \\ \frac{ic}{\rho\omega} \cdot \frac{-1}{\sqrt{1-c^2/(\rho^2\omega^2)}} \end{cases} = \frac{ic}{\rho\omega} \cdot \gamma'$, where $\gamma' = \frac{\pm 1}{\sqrt{1-\frac{c^2}{\rho^2\omega^2}}} = \frac{\pm 1}{\sqrt{1-\frac{\rho_c^2}{\rho^2}}}$, and $i = \sqrt{-1}$. Thus,

$$\frac{\gamma}{\gamma'} = \frac{ic}{\rho\omega} = \frac{i\rho_c}{\rho} \tag{5}$$

Then, (4) can be expressed as:

$$\begin{cases} ds = \gamma ds' + \gamma' icdt' \\ icdt = \gamma icdt' - \gamma' ds' \end{cases} \quad (6)$$

We denote (6) in complex number form:

$$[ds, icdt] = [\gamma ds' + \gamma' icdt', \gamma icdt' - \gamma' ds'] \quad (7)$$

Then, we have the property of each component shown in Table I.

TABLE I
COMPONENTS PROPERTY

	γ	γ'	$\gamma ds' + \gamma' icdt'$	$\gamma icdt' - \gamma' ds'$
ICC	Real	Imaginary	Real	Imaginary
OCC	Imaginary	Real	Imaginary	Real

By equating the real and imaginary parts on both sides of (7), we obtain the following:

$$\begin{cases} ds = \overset{ICC}{\longleftarrow} \gamma ds' + \gamma' icdt' \overset{OCC}{\longrightarrow} = icdt \\ icdt = \overset{ICC}{\longleftarrow} \gamma icdt' - \gamma' ds' \overset{OCC}{\longrightarrow} = ds \end{cases} \quad (8)$$

From (8), for OCC, the spatial component (γds'+γ'icdt') in frame A' is transformed to time of frame A, while the time component (γicdt'-γ'ds') in frame A' is transformed to the spatial component of frame A. This phenomenon represents a newly discovered natural law, which we refer to as "space-time exchange."

By substituting $\gamma = \gamma' ic/(\rho\omega)$ to (8), for OCC, we obtain:

$$\begin{cases} ds = -\gamma' \left[ds' + \frac{c^2}{\rho\omega} dt'\right] \\ dt = \gamma' \left[dt' + \frac{1}{\rho\omega} ds'\right] \end{cases} \quad (9)$$

Similarly, using (1), we can derive the corresponding transformation for the OCC as follows:

$$\begin{cases} ds' = \gamma' \left[ds' - \frac{c^2}{\rho\omega} dt\right] \\ dt' = -\gamma' \left[dt' - \frac{1}{\rho\omega} ds\right] \end{cases} \quad (10)$$

However, in order for (9) and (10) to form a valid pair of transformations, the following principle must be upheld: a pair of old coordinates $(ds,dt)_{old}$ is first transformed into (ds', dt') using (10), then this (ds', dt') is transformed to $(ds,dt)_{new}$ by (9), which must be equal to the original $(ds,dt)_{old}$.

To preserve this principle, we add subscripts 1, 2, 3, and 4 to γ' in (9) and (10), resulting in the following:

$$\begin{cases} ds = -\gamma_1'(ds' + \frac{c^2 dt'}{\rho\omega}) \\ dt = \gamma_2'(\frac{ds'}{\rho\omega} + dt') \end{cases}, \text{ and } \begin{cases} ds' = \gamma_3'(ds - \frac{c^2 dt}{\rho\omega}) \\ dt' = \gamma_4'(\frac{ds}{\rho\omega} - dt) \end{cases}$$

We then the transformations in matrix form as follows:

$$\begin{bmatrix} ds \\ dt \end{bmatrix} = \begin{pmatrix} -\gamma_1' & -\gamma_1' c^2/(\rho\omega) \\ \gamma_2'/(\rho\omega) & \gamma_2' \end{pmatrix} \begin{bmatrix} ds' \\ dt' \end{bmatrix},$$
$$\begin{bmatrix} ds' \\ dt' \end{bmatrix} = \begin{pmatrix} \gamma_3' & -\gamma_3' c^2/(\rho\omega) \\ \gamma_4'/(\rho\omega) & -\gamma_4' \end{pmatrix} \begin{bmatrix} ds \\ dt \end{bmatrix}$$

Since $(ds,dt)_{new}$ must be equal to $(ds,dt)_{old}$, we have:

$$\begin{bmatrix} ds \\ dt \end{bmatrix} = \begin{pmatrix} -\gamma_1' & -\gamma_1' c^2/(\rho\omega) \\ \gamma_2'/(\rho\omega) & \gamma_2' \end{pmatrix} \begin{pmatrix} \gamma_3' & -\gamma_3' c^2/(\rho\omega) \\ \gamma_4'/(\rho\omega) & -\gamma_4' \end{pmatrix} \begin{bmatrix} ds \\ dt \end{bmatrix}$$

It means:

$$\begin{pmatrix} -\gamma_1' & -\frac{\gamma_1' c^2}{\rho\omega} \\ \frac{\gamma_2'}{\rho\omega} & \gamma_2' \end{pmatrix} \begin{pmatrix} \gamma_3' & -\frac{\gamma_3' c^2}{\rho\omega} \\ \frac{\gamma_4'}{\rho\omega} & -\gamma_4' \end{pmatrix} = \begin{pmatrix} 1 & 0 \\ 0 & 1 \end{pmatrix}$$

Solving this equation yields the following result:

$$\gamma_{\prime}' = -\gamma_2' = -\gamma_3' = \gamma_4'$$

Let $\gamma_{\prime}' = -\gamma_2' = -\gamma_3' = \gamma_4' = |\gamma'|$ and -$|\gamma'|$ separately. This leads to two sets of Lorentz transformations and their inverses for the OCC, which are as follows:

Group 1: Transformation:

$$\begin{cases} ds' = -|\gamma'| \left(ds - \frac{c^2 dt}{\rho\omega}\right) \\ dt' = -|\gamma'| \left(dt - \frac{ds}{\rho\omega}\right) \end{cases} \quad (11a)$$

Inverse Transformation:

$$\begin{cases} ds = -|\gamma'| (ds' + \frac{c^2 dt'}{\rho\omega}) \\ dt = -|\gamma'| (dt' + \frac{ds'}{\rho\omega}) \end{cases} \quad (11b)$$

Group 2: Transformation

$$\begin{cases} ds' = |\gamma'| \left(ds - \frac{c^2 dt}{\rho\omega}\right) \\ dt' = |\gamma'| \left(dt - \frac{ds}{\rho\omega}\right) \end{cases} \quad (12a)$$

Inverse Transformation:

$$\begin{cases} ds = -|\gamma'| (ds' + \frac{c^2 dt'}{\rho\omega}) \\ dt = -|\gamma'| (dt' + \frac{ds'}{\rho\omega}) \end{cases} \quad (12b)$$

The inverse transformations of the tangential velocity given by these two groups are the same:

$$u_s = \frac{ds}{dt} = \frac{ds' + \frac{c^2 dt'}{\rho\omega}}{dt' + \frac{ds'}{\rho\omega}} = \frac{\frac{ds'}{dt'} + \frac{c^2}{\rho\omega}}{1 + \frac{ds'}{dt'}\frac{1}{\rho\omega}} = \frac{u_s' + \frac{c^2}{\rho\omega}}{1 + \frac{u_s'}{\rho\omega}} \quad (13)$$

If the event point is fixed in frame A', i.e., $u_s' = 0$, then the tangential velocity in frame A is given by:

$$u_s = \frac{c^2}{\rho\omega} = c \cdot \frac{\rho_c}{\rho} \tag{14}$$

Thus, the tangential velocity of frame A in the OCC is no longer $\rho\omega$, but instead $c \cdot \rho_c/\rho$, which remains less than the speed of light $c$and is inversely proportional to the radial distance ρ

Quantum mechanics postulates that the electron's spin is intrinsic because the classical analogy to rotational motion falls apart when the tangential velocity of the electron's surface is calculated using the relation $= r\omega$ implied by such a spin. For example, using classical mechanics, if we apply the equation $\frac{2}{5}mr^2\omega = \hbar/2$ (where m, r, and ω represent the mass, radius, and angular velocity of the electron, and h is the reduced Planck constant), the tangential velocity, according to $v = r\omega$, becomes superluminal. For an electron radius of 0.88×10^{-15} m, this yields a tangential velocity of v =1.644×10^{11} m/s, which exceeds the speed of light.

However, according to $\frac{2}{5}mr^2\omega = \hbar/2$, ω is $1.65 \times 10^{26}\ rad/s$, then, the corresponding ρ_c is 1.82×10^{-18} m in the OCC regime (where $\rho_c = 1.82 \times 10^{-18}\ m \ll \rho = 0.88 \times 10^{-15}\ m$), leads to a tangential velocity of v = 6.41×10^5 m/s, which is not superluminal and is consistent with the result from (14).

When the point is fixed in frame A', such that ds'= 0, (8) becomes:

$$\begin{cases} ds = \overset{ICC}{\leftarrow} \gamma' i c dt' \overset{OCC}{\longrightarrow} = icdt \\ icdt = \overset{ICC}{\leftarrow} \gamma i c dt' \overset{OCC}{\longrightarrow} ds \end{cases}$$

The tangential velocity of this point relative to frame A is given by:

For ICC:

$$\frac{ds}{dt} = \frac{\gamma' ic}{\gamma} = \rho\omega = c\frac{\rho}{\rho_c}$$

For OCC:

$$\frac{ds}{dt} = \frac{\gamma i c dt'}{\gamma' dt'} = \frac{\pm|\gamma'|(-c^2)}{\gamma'\rho\omega} = \begin{cases} \frac{c^2}{\rho\omega}, \gamma' = -|\gamma'| \\ -\frac{c^2}{\rho\omega}, \gamma' = |\gamma'| \end{cases}$$

According to (14), $u_s = \frac{c^2}{\rho\omega}$, it follows that the γ'must be $-|\gamma'|$. Therefore, we define the following relationships:

$$v(\rho) = \begin{cases} c \cdot \frac{\rho}{\rho_c}, \rho < \rho_c \\ c \cdot \frac{\rho_c}{\rho}, \rho > \rho_c \end{cases}$$

$$\gamma(\rho) = \begin{cases} \frac{1}{\sqrt{(1-\rho^2/\rho_c^2)}}, \rho < \rho_c \\ \frac{-1}{\sqrt{(1-\rho_c^2/\rho^2)}}, \rho > \rho_c \end{cases} \tag{15}$$

The unified form of Lorentz transformation for rotational frames, applicable to at both ICC and OCC is given by:

$$\begin{cases} ds' = \gamma(\rho)(ds - v(\rho)dt) \\ d\rho' = d\rho \\ dz' = dz \\ dt' = \gamma(\rho)\left(dt - \frac{v(\rho)}{c^2}ds\right) \end{cases} \tag{16}$$

and the inverse transformation is:

$$\begin{cases} ds = \gamma(\rho)(ds' + v(\rho)dt') \\ d\rho = d\rho' \\ dz = dz' \\ dt = \gamma(\rho)\left(dt' + \frac{v(\rho)}{c^2}ds'\right) \end{cases} \tag{17}$$

Using (17), we can derive the transformations for other physical quantities. Below are some examples of such transformations [4], [5]:

Mass:

$$m = \gamma(\rho)m'\left(1 + \frac{u_s' v(\rho)}{c^2}\right) \tag{18}$$

Energy:

$$w = \gamma(\rho)(w' + v(\rho)p_s') \tag{19}$$

Tangential momentum:

$$p_s = \gamma(\rho)\left(p_s' + \frac{v(\rho)w'}{c^2}\right) \tag{20}$$

Radial force F_ρ, axial force F_z and their composition force F_R:

$$F_{\rho\backslash z\backslash R} = \frac{F'_{\rho\backslash z\backslash R}}{\gamma(\rho)\left[1+\frac{u_s' v(\rho)}{c^2}\right]} = F'_{\rho\backslash z\backslash R}\gamma(\rho)\left[1 - \frac{u_s v(\rho)}{c^2}\right] \tag{21}$$

where u_s and u_s' are the tangential velocity of the acceptor in frame A and A', respectively.

IV. Critical Cylinder Effect of Electric Force

The transformations of space-time coordinates, mass, energy-momentum, and force all involve the factor γ(ρ) or its inverse, 1/γ(ρ). Importantly, γ(ρ) is negative in the OCC and positive in the ICC. As a result, these physical quantities are negative in the OCC and positive in the ICC. This represents a crucial and previously unrecognized relativistic effect, which we refer to as the CCE. Here, we specifically discuss the CCE related to the electric force acting on a spin-charged particle.

Let us assume that a charged particle, q_1, is at rest in the laboratory frame but spins around the z-axis with angular velocity ω at the origin, O, as depicted in Fig. 6. The test charge, q_2, is located at point P, and the distance from $q_1$to $q_2$is given by: $R = (\rho^2 + z^2)^{1/2}$. We treat the laboratory as frame A, and the spin of q_1 as frame A' . In frame A', the particle q_1 has no displacement or rotation and is truly at rest. The force exerted by q_1 on the test charge q_2 is the real electrostatic force, denoted F_R', and is independent of the motion of q_2 . According

to (21), when F_R' is transformed into frame A, we obtain:

$$F_R = \frac{F_R'}{\gamma(\rho)\left[1+\frac{u_s' v(\rho)}{c^2}\right]} = F_R'\gamma(\rho)\left[1-\frac{u_s v(\rho)}{c^2}\right] \quad (22)$$

where u_s' and u_s are the tangential velocities of q_2 relative to the spin of q_1 in frames A' and A, respectively. This equation implies that in frame A, the force acting on q_2 due to the spin of q_1 depends on the motion of q_2. If q_2 is stationary in frame A, i.e., u_s = 0, then (22) simplifies to

$$\frac{F_R}{F_R'} = \gamma(\rho) = \begin{cases} \left(1-\frac{\rho^2}{\rho_c^2}\right)^{-\frac{1}{2}} \\ -\left(1-\frac{\rho_c^2}{\rho^2}\right)^{-\frac{1}{2}} \end{cases} \quad (23)$$

This relationship is referred to as the first kind of CCE. It indicates that the direction of F_R will change when q_2 moves from the ICC to the OCC. Furthermore, as $\rho \to \rho_c$, F_R becomes significantly stronger, as illustrated in Fig. 7. This provides an explanation for the strong interaction observed between protons in the nucleus. Since the strong force is only significant at a distance of approximately 10^{-15} m [6], this suggests that the critical radius of a proton's spin is on the order of 10^{-15} m.

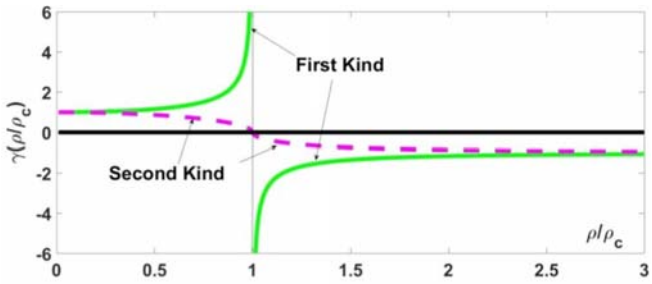

Fig. 7 Two kinds of CCEs

If q_2 is synchronously rotating with the q_1, that is, $u_s' = 0$, then (22) simplifies to:

$$F_R = \frac{F_R'}{\gamma(\rho)} \quad (24)$$

This represents the second kind of CCE. It implies that as $\rho \to \rho_c$, F_R becomes very weak. Additionally, when q_2 moves from the ICC to the OCC, F_R will cross zero and change direction, as depicted in Fig. 7. This phenomenon is responsible for what is commonly referred to as the weak interaction.

V. Explanation of Experimental Results

A. Incompletion of Coulomb's Law

Coulomb's law, which describes the electrostatic force, was discovered in the 1780s, long before the concept of electron spin was introduced [7]. Therefore, Coulomb's force is not entirely static, as it is expressed in the laboratory frame, rather than the spin frame in which the true electrostatic force, denoted as F_R' , resides. For clarity, we define Coulomb's force as F_c.

The Coulomb's law is only valid for the distance of $R > 10^{-12}$ m where $\gamma(\rho)$ = -1. The relationship between F_R' and F_c is expressed as:

$$F_R' = \frac{F_c}{\gamma(\rho)} = -\frac{q_1 q_2}{4\pi\epsilon_0 R^2} \quad (25)$$

where, F_c is:

$$F_c = \frac{q_1 q_2}{4\pi\epsilon_0 R^2} \quad (26)$$

From (25), we can conclude the following for F_R':

(a) Particles with the same sign repel each other, while particles with opposite signs attract.

(b) F_R' has the same magnitude as F_c, Same quantity as F_c, but its sign is reversed relative to that of F_c.

Furthermore, when ρ is very close to ρ_c, (26) is no longer valid for F_c, and must be modified as:

$$F_c = -\frac{q_1 q_2}{4\pi\epsilon_0 R^2}\gamma(\rho) \quad (27)$$

In general, if q_2 is neither at rest nor synchronously rotating with q_1 (i.e., $us \neq v(\rho) \neq 0$), F_c can be expressed in two parts according to (22):

$$F_c = F_R'\gamma(\rho) - F_R'\gamma(\rho)\frac{u_s v(\rho)}{c^2} = F_e + F_m \quad (28)$$

where, F_e is the electric force:

$$F_e = F_R'\gamma(\rho) = -\frac{q_1 q_2}{4\pi\epsilon_0 R^2}\gamma(\rho) = q_2 E_s \quad (29)$$

where, E_s is the electric field of q_1:

$$E_s = -\frac{q_1}{4\pi\epsilon_0 R^2}\gamma(\rho) \quad (30)$$

and F_m is the magnetic force:

$$F_m = -F_R'\gamma(\rho)\frac{u_s v(\rho)}{c^2} = \frac{q_1 q_2}{4\pi\epsilon_0 R^2}\gamma(\rho)\frac{u_s v(\rho)}{c^2} = q_2 B_s \quad (31)$$

where, B_s is the magnetic field of q_1:

$$B_s = \frac{q_1}{4\pi\epsilon_0 R^2}\gamma(\rho)\frac{u_s v(\rho)}{c^2} = \frac{q_1}{4\pi R^2}\mu_0\gamma(\rho)u_s v(\rho) \quad (32)$$

Let the ratio $v(\rho)/c^2$ be represented by the vector V, Consequently, the spin magnetic field produced by the charge q can be expressed as $B_s = V \times E_s$. This allows us to formulate the Lorentz force acting on a test charge q_2 with velocity V, due to the presence of q_1 as $F_R = q_2(E_s + V \times B_s)$.

For protons, with q_1 being 1.602×10^{-19} C, at the location R = ρ = $0.999\rho_c$, B_s is 1.07×10^{14} Tesla. At the location R = ρ = $1.001\rho_c$, B_s is $-1.08*10^{14}$ T. Thus, in laboratory frame, the spin-only q_1 possesses both electric field E_s and magnetic field B_s. Near the critical radius, B_s reaches magnitudes on the order of 10^{14} Tesla and change direction from ICC to OCC. This magnetic field cannot be accounted for by the spin magnetic

moment alone. On the other hand, Coulomb's electric field is neither the true electrostatic field nor does it fully represent the electric field E_s of spinning charged particle. Instead, it only captures a component of E_s when $\rho >> \rho_c$.

Note that the u_s in (22) represents the tangential component of the velocity u of q_2 relative to the spin of q_1 in frame A. Even if u remains constant, a change in the direction of the spin axis of q_1 will result in a different value for u_s and consequently alter the force acting on q_2. This results in a natural shift in the trajectory of q_2'. Without controlling the orientation of q_1's spin axis, the future position of q_2 is becomes inherently uncertain. This uncertainty gives rise to the probabilistic wave behavior of particles, a fundamental concept in quantum mechanics.

B. The Explanation of Our Experimental Result

Let q_1 be spinning and undergoing precession, while q_2 (ink) is spinning only. To calculate F_c, we must transform F_R' from the spin frame to the procession frame, then to the laboratory frame:

$$F_c = F_s\gamma(\rho)\gamma(r)\left[1-\frac{v(\rho)u_{sp}'}{c^2}\right]\left[1-\frac{v(r)u_{pl}}{c^2}\right] \tag{33}$$

where, for spin frame:

$$v(\rho)=\begin{cases}\rho\omega_s', \rho<\frac{c}{\omega_s'}=\rho_c\\ \frac{c^2}{\rho\omega_s'}, \rho>\frac{c}{\omega_s'}=\rho_c\end{cases}, \gamma(\rho)=\begin{cases}\frac{1}{\sqrt{1-(\frac{v(\rho)}{c})^2}}, \rho<\rho_c\\ -\frac{1}{\sqrt{1-\left(\frac{v(\rho)}{c}\right)^2}}, \rho>\rho_c\end{cases}$$

for precession frame:

$$v(r)=\begin{cases}r\omega_m, r<\frac{c}{\omega_m}=r_c\\ \frac{c^2}{r\omega_m}, r>\frac{c}{\omega_m}=r_c\end{cases}, \gamma(r)=\begin{cases}\frac{1}{\sqrt{1-(\frac{r}{r_c})^2}}, r<r_c\\ -\frac{1}{\sqrt{1-(\frac{r_c}{r})^2}}, r>r_c\end{cases}$$

Here, ρ and r represent the radial distance of the spin axis and procession axis from q_1 to q_2, respectively; ρ_c and r_c are the critical radius for the spin and precession frame, respectively; u_{sp}' and u_{pl} are the tangential velocity of q_2 with respect to the precession frame and laboratory frame of q_1, respectively; ω_s' and ω_m are the angular velocity of q_1 in spin frame and precession frame, respectively.

Since $v(\rho) \ll c$, $v(r) \ll c$, and the diffusion velocity of ink is much smaller than the tangential velocity of precession, such that $u_{sp}' \approx 0$ and $u_{pl} \approx 0$, we have:

$$F_c = F_R'\gamma(\rho)\gamma(r) = -\frac{q_1q_2}{4\pi\epsilon_0R^2}\gamma(\rho)\gamma(r) \tag{34}$$

For our laboratory experiment, we take $\rho_c \approx 10^{-18}\ m$ and $r_c \approx 1.5\times10^{-2}\ m$. For the ink, it is at the OCC of the spin frame (R>1*$10^{-18}\ m$), that is, $\gamma(\rho) \approx -1$, then we have:

$$F_c \approx -F_R'\gamma(r) = \frac{q_1q_2}{4\pi\varepsilon_0R^2}\gamma(r) \tag{35}$$

Now, for the ink on the right side of the red line (i.e., $R = r > r_c$), it resides in the OCC of pression frame where $\gamma(r) < 0$, resulting in $F_c < 0$. This causes the ink to be attracted toward the left. Conversely, for the ink located to the left of the red line (i.e., $R = r < r_c$); it resides in the ICC of the pression frame where $\gamma(r) > 0$, leading to $F_c > 0$. This causes the ink to be repelled to the right. Ultimately, the ink remains in the region near the critical radius.

VI. Masses of Proton and Electron

To calculate the gravitational force exerted by the Earth on a body located outside its surface, we often simplify the Earth's mass distribution by assuming that its total mass M is concentrated at its center. This approximation allows us to treat the Earth as a point mass, which simplifies the gravitational force calculation. The same principle applies when analyzing the external properties of a spinning charged particle. Although the internal structure of the particle may be complex, we can model its charge q as uniformly distributed within a spherical volume of radius b. This simplification is valid for many cases, particularly when the particle's internal dynamics do not significantly affect its external fields.

We consider the laboratory as reference frame A and the spin of the particle as reference frame A'. In frame A', the particle is at rest, and its electric field corresponds to the true electrostatic field generated by the particle. To determine the value of this electrostatic field at a distance r from the center of the particle, we can use the assumption of a uniform charge distribution. This allows us to apply Gauss's Law to calculate the electric field:

$$E_r' = \begin{cases}-kqr/b^3, r<b\\ -kq/r^2, r>b\end{cases} \tag{35}$$

where $k = 1/(4\pi\varepsilon_0)$.

The field energy w' at that point is:

$$w'(r) = (\varepsilon_0/2)E_r'^2 = \begin{cases}(\varepsilon_0/2)k^2q^2r^2/b^6 & r<b\\ (\varepsilon_0/2)k^2q^2/r^4 & r>b\end{cases} \tag{36}$$

To obtain the total field energy of the charged particle in its spinning reference frame, we must integrate the energy density $w'(r)$ over the entire three-dimensional space. This integral is performed in spherical coordinates (r, φ, θ) where r is the radial distance from the center of the particle, and φ and θ are the angular coordinates.

The total energy within the charged ball (denoted as W_i') is the sum of the energy contained in the region inside the ball ($r < b$):

$$W_i' = \frac{\varepsilon_0k^2q^2}{2b^6}\int_0^{2\pi}d\varphi\int_0^{\frac{\pi}{2}}sin\theta d\theta\int_0^b 2r^4dr = \frac{kq^2}{10b} \tag{37}$$

The total energy outside the charged ball (denoted as W_o') is

the sum of the energy contained in the region outside the ball ($r > b$):

$$W_o' = \frac{\varepsilon_0 k^2 q^2}{2} \int_0^{2\pi} d\varphi \int_0^{\frac{\pi}{2}} sin\theta d\theta \int_b^{\infty} \frac{2}{r^2} dr = \frac{kq^2}{2b} \quad (38)$$

Similarly, the energy outside the spherical charge distribution (for $r > a$, where $a > b$) is denoted as W_{ao}' and it can be expressed as:

$$W_{ao}' = \frac{kq^2}{2a} \quad (39)$$

If a is 1000 times b ($a = 1000b$), then W_{ao}' is 0.001 times W_o'. This suggests that 99.9% of the energy outside the charged ball is confined within a ball of radius a equal to 1000 times b. Conversely, if $a = 2b$, then $W_{ao}' = W_o'/2$, indicating that half of the energy outside the charged ball is located within the spherical shell defined by $b < r < 2b$.

The total field energy in the spinning frame, denoted as W', is the sum of W_i' and W_o':

$$W' = W_i' + W_o' = \frac{1.2kq^2}{2b} \quad (40)$$

For a proton, the charge q is 1.602×10^{-19}C. If the radius b is 0.9194×10^{-18} m, then the total field energy W' is 1.5053×10^{-10} J. This energy corresponds to the rest mass of the proton, m', which can be calculated using the relationship $m' = \frac{W'}{c^2} = 1.67252 \times 10^{-27}$ kg. This result leads to the idea that "mass arises from its field energy" and suggests that the particle's field energy in the spinning frame is a single, definite value, lacking quantum properties.

From the above discussion, we can deduce the radius of the equivalent charge distribution as follows:

$$b = 0.6ke^2/W'' = 0.9194*10^{-18}\,\text{m}$$

In the context of energy-momentum transformation, the relationship is given by:

$$w = \gamma(\rho)(w' + v(\rho)p_s') \quad (41)$$

where the momentum in the spinning frame, p_s', is zero ($p_s' = 0$). Consequently, the field energy at a point located a distance $r = \sqrt{\rho^2 + z^2}$ from the center of the charged ball in the laboratory frame can be expressed as follows:

$$w(\rho) = \begin{cases} \frac{\gamma(\rho)\left(\frac{\varepsilon_0}{2}\right)k^2q^2r^2}{b^6} & r < b \\ \frac{\gamma(\rho)\left(\frac{\varepsilon_0}{2}\right)k^2q^2}{r^4} & r > b \end{cases} \quad (42)$$

where

$$\gamma(\rho) = \begin{cases} \frac{1}{\sqrt{1-(\frac{\rho}{\rho_c})^2}}, \rho < \rho_c \\ -\frac{1}{\sqrt{1-\left(\frac{\rho_c}{\rho}\right)^2}}, \rho > \rho_c \end{cases}$$

The total field energy of a spinning charged particle in the laboratory frame is obtained by integrating the energy at each point, $w(\rho)$, over the entire three-dimensional space. However, since $w(\rho)$ depends on γ(ρ) and the expression for γ(ρ) differs between the ICC and OCC, this integration must be divided into four distinct parts:

(A) W_1 for the region where $b < \rho < \rho_c$
(B) W_2 for the region where $\rho_c < \rho < \infty$
(C) W_3 for the region where $\rho < b, z > \sqrt{b^2 - \rho^2}$
(D) W_4 for the region where $\rho < b, z < \sqrt{b^2 - \rho^2}$

These regions are illustrated in Fig. 8.

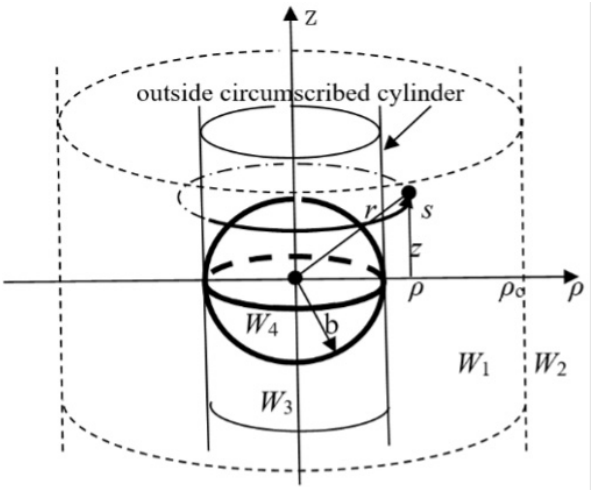

Fig. 8 Charge Ball and Critical Cylinder

A. Energy for the Region $b < \rho < \rho_c$, Calculation of W_1

For the region $b < \rho < \rho_c$, the energy W_1 is given by

$$W_1 = \frac{\varepsilon_0 k^2 q^2}{2} \int_b^{\rho_c} \frac{d\rho}{\sqrt{1-\rho^2/\rho_c^2}} d\rho \int_0^{2\pi\rho} ds \int_0^{\infty} \frac{2dz}{(\rho^2+z^2)^2} \quad (43)$$

Note that:

$$\int_0^{\infty} \frac{dz}{(\rho^2+z^2)^2} = \left[\frac{z}{2\rho^2(\rho^2+z^2)} + \frac{\arctan\left(\frac{z}{\rho}\right)}{2\rho^3}\right]_0^{\infty} = \frac{\pi(n\pm\frac{1}{2})}{2\rho^3}, n = 0,1,2,\cdots$$

Thus, W_1becomes:

$$W_1 = \frac{kq^2}{4}\pi\left(n \pm \frac{1}{2}\right) \int_b^{\rho_c} \frac{\rho_c d\rho}{\rho^2\sqrt{\rho_c^2-\rho^2}} d\rho$$

Evaluating this integral gives:

$$W_1 = \frac{kq^2}{2b}\frac{\pi}{2}\left(n \pm \frac{1}{2}\right)\sqrt{1-\frac{b^2}{\rho_c^2}}, \text{n} = 0,1,2,\cdots \quad (44)$$

B. Energy for the Region $\rho_c < \rho < \infty$, Calculation of W_2

For the region of OCC, $\rho_c < \rho < \infty$, W_2 is given by:

$$W_2 = \frac{\varepsilon_0 k^2 q^2}{2}\int_0^{2\pi\rho} ds \int_{\rho_c}^{\infty} -(1-\rho_c^2/\rho^2)^{-1/2}\, d\rho \int_0^{\infty} \frac{2dz}{(\rho^2+z^2)^2}.$$

Simplifying using the same z-integral result as before:

$$W_2 = \frac{kq^2}{4}\pi\left(n \pm \frac{1}{2}\right)\int_{\rho_c}^{\infty} \frac{-d\rho}{\rho\sqrt{\rho^2-\rho_c^2}}$$

Solving the integral gives:

$$W_2 = -\frac{kq^2\pi\left(n\pm\frac{1}{2}\right)}{4}\left(\frac{arccos(\rho_c/\rho)}{\rho_c}\right)\Big|_{\rho_c}^{\infty}$$

This simplifies further to:

$$W_2 = -\frac{kq^2\pi^2}{4\rho_c}\left(n \pm \frac{1}{2}\right)\left(m \pm \frac{1}{2}\right), \quad n = 0,1,2,,\cdots, m = 0,1,2,\cdots \quad (45)$$

The total energy outside the circumscribed cylinder of the charged ball in the laboratory frame is obtained by summing the contributions from W_1 and W_2:

$$W_1 + W_2 = \frac{kq^2}{2b}\frac{\pi}{2}\left\{\sqrt{1-\frac{b^2}{\rho_c^2}} - \frac{b\pi}{\rho_c}\left(m \pm \frac{1}{2}\right)\right\}\left(n \pm \frac{1}{2}\right), n = 0,1,2,\cdots, m = 0,1,2,\cdots \quad (46)$$

This implies that the energy of a spinning charged particle in the laboratory frame has multiple possible values, which in turn means that the particle's mass also exhibits multiple discrete values. This characteristic is identified as the quantum property of a spinning particle. Evidently, this quantum property is a direct consequence of the CCE.

The term $\left(n \pm \frac{1}{2}\right), n = 0,1,2, \ldots.$, incorporates both the principal quantum number n and the spin quantum number $s = \pm\frac{1}{2}$, which arise from the discrete energy states of the spinning charged particle. Simultaneously, the factor $\left(m \pm \frac{1}{2}\right), m = 0,1,2, \ldots$, accounts for the Zeeman splitting, which describes the energy-level splitting under the influence of a magnetic field, as discussed in [8].

C. Energy for the Region $\rho < b, z > \sqrt{b^2-\rho^2}$, Calculation of W_3

The energy within the circumscribed cylinder of the charged ball, but outside the charged ball itself is:

$$W_3 = \frac{\varepsilon_0 k^2 q^2}{2}\int_0^b \gamma(\rho) d\rho \int_0^{2\pi\rho} ds \int_{\sqrt{b^2-\rho^2}}^{\infty} \frac{2dz}{(\rho^2+z^2)^2} \quad (47)$$

However, it is important to note that this expression does not have a closed-form analytic solution and must instead be evaluated numerically.

D. Energy for the Region $\rho < b, z < \sqrt{b^2-\rho^2}$, Calculation of W_4

The total energy within the charged ball is given by (48), which does not have a closed-form analytic solution either and must instead be evaluated numerically:

$$W_4 = \frac{\varepsilon_0 k^2 q^2}{2b^6}\int_0^b \frac{2d\rho}{\sqrt{1-\frac{\rho^2}{\rho_c^2}}} d\rho \int_0^{2\pi\rho} ds \int_0^{(b^2-\rho^2)^{\frac{1}{2}}} (\rho^2+z^2) dz \quad (48)$$

In addition to spin, charged particles can undergo other forms of rotational motion, such as magnetic precession and system precession. Each type of rotation is associated with its own CCE, which can lead to the energy assuming multiple discrete values. These energy variations give rise to the magnetic quantum number and angular quantum number, which are fundamental to describing the rotational dynamics of charged particles. The existence of these quantum numbers underscores the complexity of the rotational behavior of charged particles and contributes to their distinctive quantum properties.

For proton, where $\rho_c = 10^{-15}$m >> $b = 0.9194\times10^{-18}$ m, (46) can be expressed as follows:

$$W_1 + W_2 = \frac{kq^2}{2b}\frac{\pi}{2}\left\{\sqrt{1-\frac{b^2}{\rho_c^2}} - \frac{b\pi}{\rho_c}\left(m \pm \frac{1}{2}\right)\right\}\left(n \pm \frac{1}{2}\right)$$

$$W_1 + W_2 = \frac{kq^2}{2b}\frac{\pi}{2}\left(n \pm \frac{1}{2}\right), n = 0,1,2,\cdots,$$

Given that $b = 0.9194\times10^{-3}\rho_c$, $\rho_c = c/\omega_s$, (ω_s is angular velocity of spin), the quantum interval of energy is as follows:

$$\Delta W = \frac{kq^2}{2b}\frac{\pi}{2} = 1.6656\times10^{-10}(J)$$

$$\Delta W = \frac{kq^2}{4}\frac{1000\pi}{0.9194}\frac{\omega_s}{c} = (6.5683 * 10^{-34}(Js))\omega_s.$$

This indicates that the energy quantum interval ΔW is proportional to ω_s, with a proportionality constant of $6.5683 * 10^{-34}$ (Js), which corresponds to Planck's constant.

As we discussed before, the rest mass of the particle in the spin frame A' is 1.67252×10^{-27} kg. The critical radius associated with the spin of a proton is approximately $\rho_c = 10^{-15}$ m, which is more than a thousand times larger than b. As a result, over 99.9% of the proton's energy or mass is contained within ICC. This significant concentration allows us to neglect the minimal mass present in the OCC and the effects of the CCE on the proton's mass. Furthermore, because ρ_c i is substantially larger than b, we can regard $\gamma(\rho)$ is approximately 1 in the ICC. Consequently, the total field energy of the proton in the laboratory frame is nearly identical to that in its spin frame, resulting in its mass in the laboratory frame being almost equal to its rest mass in the spin frame, which is $1.67252 * 10^{-27}$ kg.

In contrast, the critical radius for an electron's spin is approximately 10^{-18} meters, closely aligned with the charge radius. This proximity necessitates considering the field energy of the electron in both the ICC and the OCC. The total energy in the OCC is not only multivalued but also negative (because of the negative $\gamma(\rho)$), allowing it to offset the positive energy in the ICC. Assuming the radius of the electron's charged ball is the same as that of the proton, due to their identical absolute charge, the critical radius for the electron's spin should be ρ_c =

$1.16*10^{-18}$ m.

In this scenario, for the state characterized by $n = 0$, m = 0, $s = 1/2$, the total energy in the OCC is:

$$W_2 = -\frac{kq^2\pi^2}{16\rho_c} = -12.266 * 10^{-11}\ (J)$$

The energy outside circumscribed cylinder of charge ball but within critical cylinder is:

$$W_1 = \frac{kq^2}{2b}\frac{\pi}{4}\sqrt{1 - b^2/\rho_c^2} = 5.91145 * 10^{-11}(J)$$

The energy within the charged ball can be determined through numerical integration,

$$W_4 = \frac{\varepsilon_0 k^2 q^2}{2b^6}\int_0^b \frac{2d\rho}{\sqrt{1-\rho^2/\rho_c^2}} d\rho \int_0^{2\pi\rho} ds \int_0^{(b^2-\rho^2)^{1/2}} (\rho^2 + z^2) dz$$
$$= 3.01*10^{-11}(J)$$

Using numerical integration, the energy within the circumscribed cylinder of the charged ball but outside the charged ball itself is calculated as follows:

$$W_3 = \frac{\varepsilon_0 k^2 q^2}{2}\int_0^b \gamma(\rho) d\rho \int_0^{2\pi\rho} ds \int_{\sqrt{b^2-\rho^2}}^{\infty} \frac{2dz}{(\rho^2+z^2)^2} = 3.35 * 10^{-11}\ (J)$$

Thus, the total energy of a spinning electron in the laboratory frame, for the state characterized by m = 0, n = 0, s = 1/2, is 8.2×10^{-14}J, which corresponds to a mass of 9.1×10^{-31} kg that is well known electron mass.

In the spin frame A', the mass of an electron is calculated as $0.6ke^2/b = 1.6725\times10^{-27}$ kg, However, in the laboratory frame A, it is 9.1×10^{-31} kg. The difference of 1.6716×10^{-27} kg is termed "dark mass," which can be partially made observable through other forms of rotational motion. This understanding not only reveals the source of quantum properties but also elucidates the origins of mass and dark mass. In the laboratory frame, mass is distributed on either side of the critical cylinder with opposite signs, effectively canceling each other out. The so-called rest mass of charged particles in the laboratory frame is merely the remainder after this cancellation, rather than the true rest mass in the spin frame. Therefore, what is termed "dark matter" is simply the portion of mass that is canceled out in the laboratory frame; it exists in the spinning frame but remains undetectable in the laboratory frame.

VII. Conclusions

Our experiment provides compelling evidence that the spin of a particle can be understood as a rotation around a fixed axis. At the OCC, space-time undergoes an exchange that ensures the tangential velocity of a spinning particle never exceeds the speed of light. Furthermore, the CCE demonstrates that many physical quantities exhibit opposite signs in the ICC compared to the OCC. This implies that Coulomb's law requires modification to accurately describe the real electrostatic force, which only exists within the spin frame.

The field energy of a spinning particle is the source of its mass. In the laboratory frame, when the critical radius is approximately a thousand times greater than the radius of the charged particle, such as the proton, this energy is concentrated within the ICC. This concentration results in the proton's mass being nearly identical in both the laboratory and spin frames. Additionally, the quantum energy interval ΔW is proportional to the spin angular velocity ω_s, with Planck's constant acting as the proportionality factor.

In contrast, the electron, being much smaller than the proton, distributes its field energy across both the ICC and the OCC in the laboratory frame. The reversal of the Lorentz factor between the ICC and OCC creates a discrepancy in the total field energy between the laboratory frame and the spin frame. This discrepancy accounts for the electron's mass being significantly smaller than the proton's mass in the laboratory frame. The difference in mass observed between the electron in the spin frame and the laboratory frame is referred to as "dark mass."

In summary, the reversal of the Lorentz factor between the ICC and OCC, driven by the CCE, is responsible for the creation of both dark matter and dark energy.

References

[1] www.youtube.com/watch?v = GJX-3AosxZk&t = 7s
[2] C.N. Yang, R.L. Mills: "Conservation of Isotopic Spin and Isotopic Gauge Invariance", pp.191-195, Physics Review (96)1,
[3] C. Moller, "The Theory of Relativity" Clarendon Press, Oxford, 1972, pp. 15–64.
[4] Yin Rui, "Rotating Lorentz Transformation and unification of Forces" BUAA Press, Beijing, 1997, pp. 123–135.
[5] Yin Rui, "Unification of Forces According to Relativity for Rotations", Hadronic Journal, Vol. 23, No. 5, October 2000.
[6] Harald Fritzsch: "QUARKS The Stuff of Matter", Basic Books, INC., Publisher, New York, 1983.
[7] G. Spavieri, et al: "Physical implications of Coulomb's Law", Metrologia, October 2004.
[8] Palsh B. Pal, An Introductory course of particle Physics", CRC press, 2015

Rui Yin graduated from electronic engineering department of Beihang University, Beijing, China in 1960. Since then, he has worked at Beihang University as lecturer, associate professor, and professor. From 1982 to 1983, as a visiting scholar presented the research work about MRI with DR. Paul Lauterbur at State University of New York at Stony Brook. The research interests are digital signal processing, MRI, and Magnetic Resonance Therapy (MRT) and relativistic effect of rotation.